Available online at www.sciencedirect.com
SCIENCE DIRECT®
Journal of Nuclear Materials 336 (2005) 225–232
journal of nuclear materials
www.elsevier.com/locate/jnucmat

Deformation microstructure of neutron-irradiated pure polycrystalline vanadium

N. Hashimoto *, T.S. Byun, K. Farrell, S.J. Zinkle

Metals and Ceramics Division, Oak Ridge National Laboratory, P.O. Box 2008, Bldg. 4500S, MS 6136, Oak Ridge, TN 37831-6136, USA

Received 23 June 2004; accepted 13 September 2004

Abstract

The deformation microstructure of irradiated pure vanadium has been investigated by transmission electron microscopy. Dislocation pileup on grain boundaries were observed in the deformed specimens irradiated to 0.012 dpa, indicating that the source of channeling could not be grain boundary only. TEM analysis suggested a relationship between tensile direction and channeling-occurred grain: there is a tendency that directions of the applied stress with greater resolved shear stress lie on the trace containing [0 1 1] and [1 1 2] directions. Channel width is wider in case the angle between tensile direction and dislocation slip direction is close to 45°. There is a dose dependence on the correlation between channel width and resolved shear stress, the slope of this correlation decreased with increasing dose. It is suggested that the loss of work hardening capacity in irradiated pure vanadium could be mainly due to dislocation channeling locally formed with high resolved shear stress.

1. Introduction

Irradiation can produce dramatic changes in the mechanical properties of metals [1–7]. Early studies on irradiated metals [3,4,8,9] clearly demonstrated that irradiation at low temperatures produced pronounced hardening. The hardening is typically accompanied by a severe decrease in uniform plastic elongation as measured in a uniaxial tensile test [1–3]. The decrease in tensile ductility associated with low temperature neutron irradiation was the topic of numerous studies performed in the 1960s, and the phenomenon was commonly referred to as the low temperature radiation embrittlement. A more appropriate term for the low uniform elongation typically observed following low temperature irradiation is the loss of strain hardening capacity. A general feature associated with irradiation at low temperature is increased matrix hardness due to the presence of radiation-induced defects which act as obstacles to dislocation motion. The yield strength increases with increasing dose up to ~0.1 displacements per atom (dpa), and then reaches an apparent saturation hardening regime where the yield strength remains nearly constant as the dose is increased. A similar low-dose rapid hardening regime followed by a slowly evolving hardening behavior at higher doses has been observed in several FCC and BCC metals irradiated at low temperatures

* Corresponding author. Tel.: +1 865 576 2714; fax: +1 865 574 0641.
E-mail address: hashimoton@ornl.gov (N. Hashimoto).

0022-3115/$ - see front matter © 2004 Elsevier B.V. All rights reserved.
doi:10.1016/j.jnucmat.2004.09.017

Table 1
Chemical composition of high-purity vanadium used and heat treatments (wt.ppm)

C	Mn	Si	Cr	Ni	W	Mo	Ti	Cu	O	N	V
24	8	260	<100	<50	66	390	<50	<50	270	96	Bal.

Heat treatment: 30 min at 900 °C.

[8–12]. The present paper will focus on the deformation microstructure, especially dislocation channeling, in a neutron-irradiated BCC metal (Vanadium) in order better to understand the deformation mechanisms of materials showing loss of strain hardening capacity.

2. Experimental procedure

High-purity polycrystalline vanadium (BCC) was obtained from Alfa Aesar Corporation. Chemical compositions and heat treatment are shown in Table 1. The average grain size was 7 μm after the heat treatment. Custom-designed sheet tensile specimens with gauge section of 8.00 mm × 0.25 mm × 1.5 mm and an overall length of 17.0 mm were irradiated in flowing coolant water in the hydraulic tube facility of the High Flux Isotope Reactor. The inlet and outlet temperature of the water is 49 °C and 69 °C, respectively. The temperature of the specimens was estimated to be in the range of 65–100 °C. The irradiation exposures ranged from 1.1×10^{21} to 6.3×10^{24} n m^{-2}, $E > 0.1$ MeV. Correspondingly, nominal atomic displacement levels ranged from 0.0001 dpa to 0.69 dpa. All tensile tests were conducted at room temperature in a screw-driven machine at a crosshead speed of 0.008 mm s^{-1}, corresponding to a specimen strain rate of 10^{-3} s^{-1}. Engineering strain was calculated from the recorded crosshead separation using a nominal gauge length of 8 mm. Engineering stress was calculated as the load divided by the initial cross section area before irradiation. The load cell was calibrated to NIST-approved standards. The 0.2% offset yield strength (YS), ultimate tensile strength (UTS), uniform elongation (E_U), and total elongation (E_t) were calculated from the engineering load–elongation curves. The TEM pieces cut from the gauge sections of the tensile specimens had dimensions of only 1.5 × 2.0 × 0.25 mm, which is much smaller than a standard 3 mm diameter TEM disk. Preparation of electrothinned foils from these small pieces in a Tenupol electropolishing apparatus required substantial development work and modification of Tenupol specimen holders, details of which are available in Ref. [12]. Electron microscopy observation was performed with the JEM-2000FX transmission electron microscope operating at 200 kV at Oak Ridge National Laboratory (ORNL). The foil thickness was measured using thickness fringes in order to quantify defect density values.

3. Results and discussion

3.1. Tensile property and deformation microstructure

Fig. 1(a) and (b) show the tensile properties of pure vanadium irradiated up to 0.69 dpa. The neutron irradiation increased the strength of vanadium by more than 70% at a maximum dose of 0.69 dpa. The YS and UTS increased gradually with increasing irradiation dose between 0.0001 and 0.1 dpa. The uniform elongation (UE) and total elongation (TE) decreased rapidly at 0.001 dpa, and less uniform elongation was shown at higher doses. The uniform elongation at 0.012, 0.12, and 0.69 dpa was 0.1%, 0.3%, and 0.1%, respectively. Fig. 2 shows scanning electron micrographs of fracture

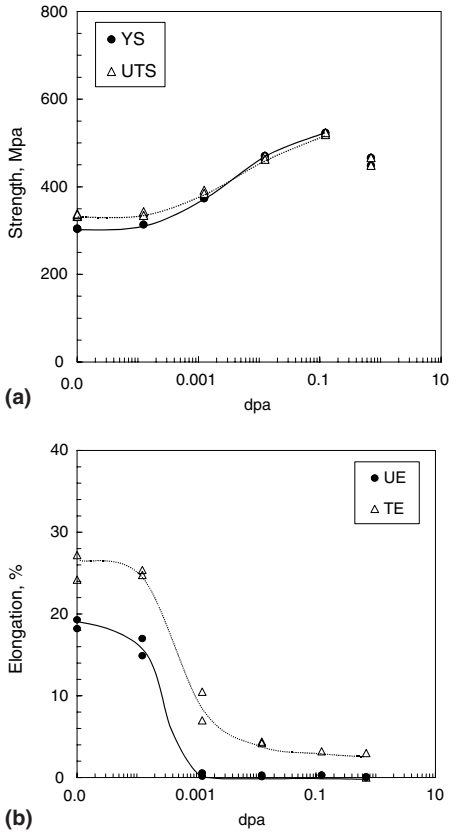

Fig. 1. Dose dependence of strength and elongation of neutron-irradiated pure vanadium.

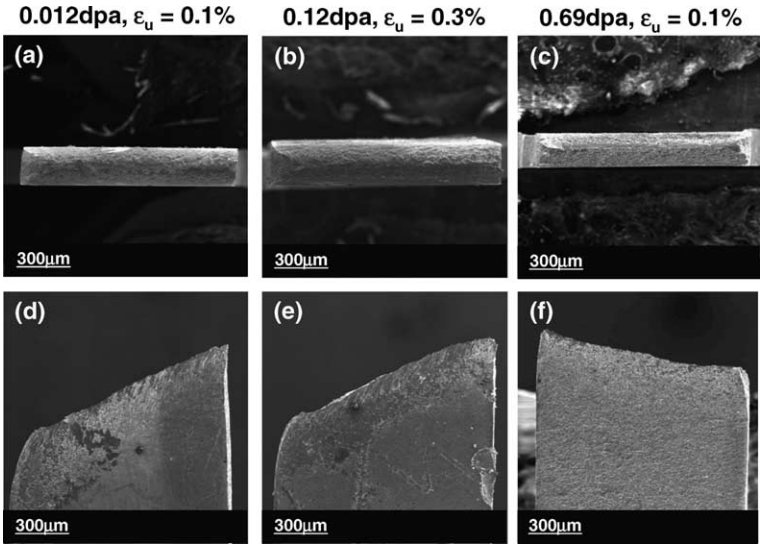

Fig. 2. Scanning electron micrographs of fracture surface of neutron-irradiated pure vanadium.

surface, indicating typical ductile tearing. Deformation microstructures of vanadium irradiated at 0.012, 0.12, and 0.69 dpa, are shown in Fig. 3. Neutron irradiation at low temperature-induced tiny defect clusters (~2 nm) with high number density (~10^{23}). The detail of defect cluster and tensile property is listed in Table 2.

From simple geometric considerations of a dislocation traversing a slip plane which intersects randomly distributed obstacles of diameter d and atomic density N, the increase in the uniaxial tensile stress for polycrystalline specimens ($\Delta\sigma$) in a pure metal is given by the well-known dispersed barrier hardening equation [5,13,14]

$$\Delta\sigma = M\alpha\mu b(Nd)^{1/2}, \tag{1}$$

where μ is the shear modulus, b is the magnitude of the Burgers vector of the glide dislocation ($\sqrt{3}a_0/2$ for BCC, where a_0 is the lattice parameter), M is the Taylor factor (3.06 for equiaxed BCC metals), and α is average barrier strength of the radiation-induced defect clusters. In this experiment, a value of $\alpha \approx 0.26$ was obtained for pure polycrystalline vanadium. Past experimental estimates range from $\alpha \sim 0.18$–0.4 for pure vanadium [15–18], 0.10–0.25 for copper [19,20], austenitic stainless steel [13,21,22], and V–4Cr–4Ti [23] irradiated at low temperatures.

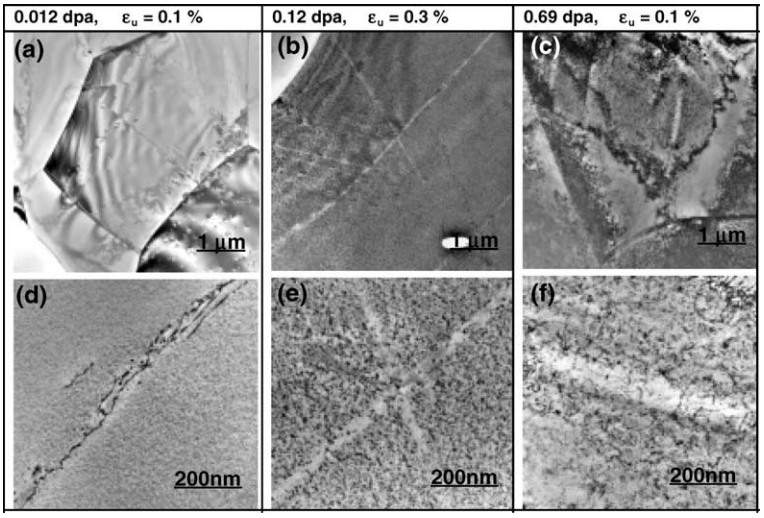

Fig. 3. Microstructure of deformed pure vanadium irradiated up to 0.69 dpa.

Table 2
Summary of defect cluster and tensile property in neutron-irradiated pure vanadium

Material	Irradiation dose (dpa)	Defect cluster			Tensile property			
		Density (m^{-3})	Size (m)	SQRT(Nd) (m^{-1})	$YS_{unirr.}$ (MPa)	$YS_{irr.}$ (MPa)	$\Delta\sigma_y$ (MPa)	UTS (MPa)
V	0.012	1.1×10^{23}	1.8×10^{-9}	1.42×10^{-7}	304	470	167	470
	0.12	1.9×10^{23}	2.1×10^{-9}	2.00×10^{-7}	304	523	219	523
	0.69	2.3×10^{23}	2.1×10^{-9}	2.18×10^{-7}	304	448	144	448

Fig. 3 shows dislocation channeling observed in each irradiation condition. Channel width varied widely (25–225 nm). Generally, not only channel width but also spacing would be one of important factors for deformation study. However, the statistics for channel spacing were too poor to attempt correlation of spacing (1–2 channels per 5–10 μm size grain), therefore only width was provided in this study. For detailed microstructural analysis of dislocation channeling, the beam direction $B \approx [\bar{1}\,1\,1]$ and [0 0 1] were selected. With an assumption that dislocations would move to ⟨1 1 1⟩direction on {1 1 2}, {1 1 0}, or {1 2 3} plane, the slip system can be geometrically determined for each channel. Channel width also can be estimated with considering the tilt angle of the slip plane. Dislocation channels tend to be on {1 1 2} planes (and only one case of {1 1 0} plane) in all irradiation conditions. In addition, curved dislocation channels were observed (Fig. 3(b)). It seemed that moving dislocations changed the slip system from $(1\,2\,1)[\bar{1}\,1\,\bar{1}]$ to $(\bar{2}\,\bar{1}\,1)[\bar{1}\,1\,\bar{1}]$. Dislocation channeling occurs because the radiation-induced defect clusters produced at low irradiation temperatures can be readily cut by gliding dislocations. This produces a defect-free path for subsequent dislocations emitted from the operating source. In general, dislocation channeling begins to occur above a critical dose/hardening level (corresponding to $N > \sim1\times10^{23}/m^3$ for copper tested at room temperature [19]). In this experiment, dislocation channeling occurred even at low dose (0.012 dpa) because irradiation-induced defect clusters were present in sufficient density ($N > 1\times10^{23}/m^3$) for dislocation channeling.

Fig. 4 shows that some residual dislocations moving in channels on {1 1 2} plane still remained in the channels after tensile test [24]. The channels with dislocations are on (1 1 2), $(\bar{1}\,\bar{1}\,2)$, and $(2\,\bar{1}\,\bar{1})$ plane and corresponding slip directions are $[\bar{1}\,\bar{1}\,1]$, [1 1 1], and $[1\,\bar{1}\,1]$, respectively. In Fig. 4(b), dislocation line-up on $(\bar{1}\,\bar{1}\,2)$ and pileup on grain boundary can be seen. Dislocation channeling has been suggested to also induce grain boundary cracking in some irradiated BCC alloys [20]. This experimental result suggested that channeling formation could lead to grain boundary cracking due to the stress localization at a source of cracking by dislocation pileup.

3.2. Effect of orientation on dislocation channeling

When tensile specimen is loaded in uniaxial tension, the applied stress, σ_{as}, is resolved on the slip planes in

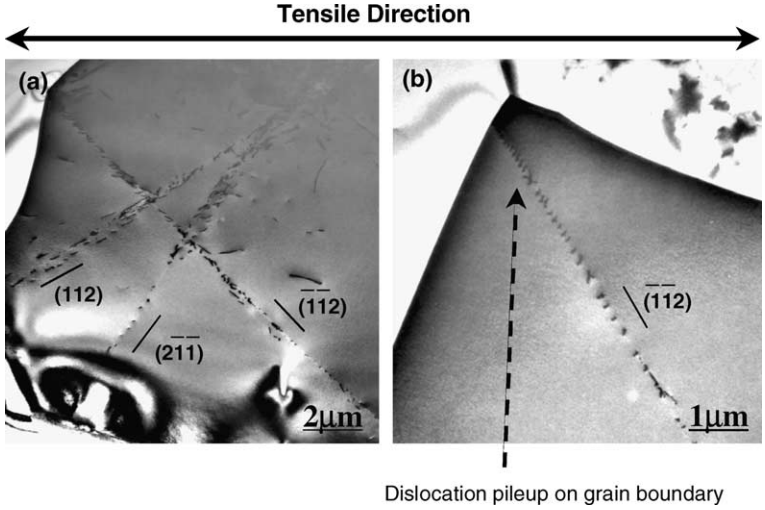

Fig. 4. Microstructure of dislocations in channels after tensile test [24]. (a) The resolved shear stress of the channels on $(\bar{1}\,\bar{1}\,2)$, $(2\,\bar{1}\,\bar{1})$ and (1 1 2) plane were estimated to be 230.2, 170.5 and 76.7 MPa, respectively, for the tensile direction $[3\,4\,\bar{1}]$.

the material. The resolved shear stress, τ_{rss}, on any given plane is determined by the angles between the plane normal and the applied stress (ϕ) and between the slip direction and the applied stress (θ): $\tau_{rss} = \sigma_{as}\cos(\phi)\cos(\theta)$. The relationship between τ_{rss} and σ_{as} is complicated by the fact that maximum resolved shear stress will vary from one grain to another. In addition, material compatibility and continuity act to limit the deformation of any one grain that may be favorably oriented by slip. In this experiment, TEM pieces were taken from the tensile specimens in rectangular shape (1.5×2.0 mm) in order to estimate the tensile axis in the TEM. To set the rectangular specimen parallel to the TEM holder, the tensile axis (the direction of applied stress) could be determined by the diffraction pattern of the grain. As described above, with using the beam direction $B \approx [\bar{1}\,1\,1]$ and [0 0 1], the slip system (slip plane normal and slip direction) can be determined for each channel. On the assumption that all of channels were formed at the yield stress ($\sigma_{as} \approx$ YS or UTS), the resolved shear stress for each dislocation channel was estimated. It was also assumed that all the grains in the material deformed uniformly and grain rotation during deformation is negligible.

Fig. 5 shows relationship between the direction of the applied stress (tensile axis) in the channeling-occurred grain and the estimated resolved shear stress for each channel. For example, the resolved shear stress of the channels on $(\bar{1}\,\bar{1}\,2)$, $(2\,\bar{1}\,\bar{1})$ and (1 1 2) plane in Fig. 4(a) were estimated to be 230.2, 170.5 and 76.7 MPa, respectively, for the tensile direction $[3\,4\,\bar{1}]$. There is a tendency that directions of the applied stress with greater resolved shear stress lie on the trace containing [0 1 1] and [1 1 2] directions.

Fig. 6 shows the dependence of angle between tensile axis and slip plane normal (a) and slip direction (b) on resolved shear stress in each channeling-occurred grain. Since maximum resolved shear stress varies from one grain to another when tensile specimen is loaded in uniaxial tension, the values of estimated resolved stress varied widely (100–260 MPa) for different dislocation channels. However, there is a tendency for the resolved shear stress to be great when the angle is around 45° in both cases. The Schmid factor, m, is defined as the ratio of the resolved shear stress to the axial stress, $m = \cos(\phi)\cos(\theta)$. The maximum value of m occurs when the shear plane is at a 45° angle to the applied stress. It should be noted that there is the same tendency as the resolved shear stress for channel width (Fig. 7). Channel width also varied widely but it exhibited an angular dependence, especially at high dose. Actually, in both cases of the resolved shear stress and channel width, the maximum value is not at 45° angle. A possible reason of this divergence would be due to the assumption that grain rotation during deformation is negligible.

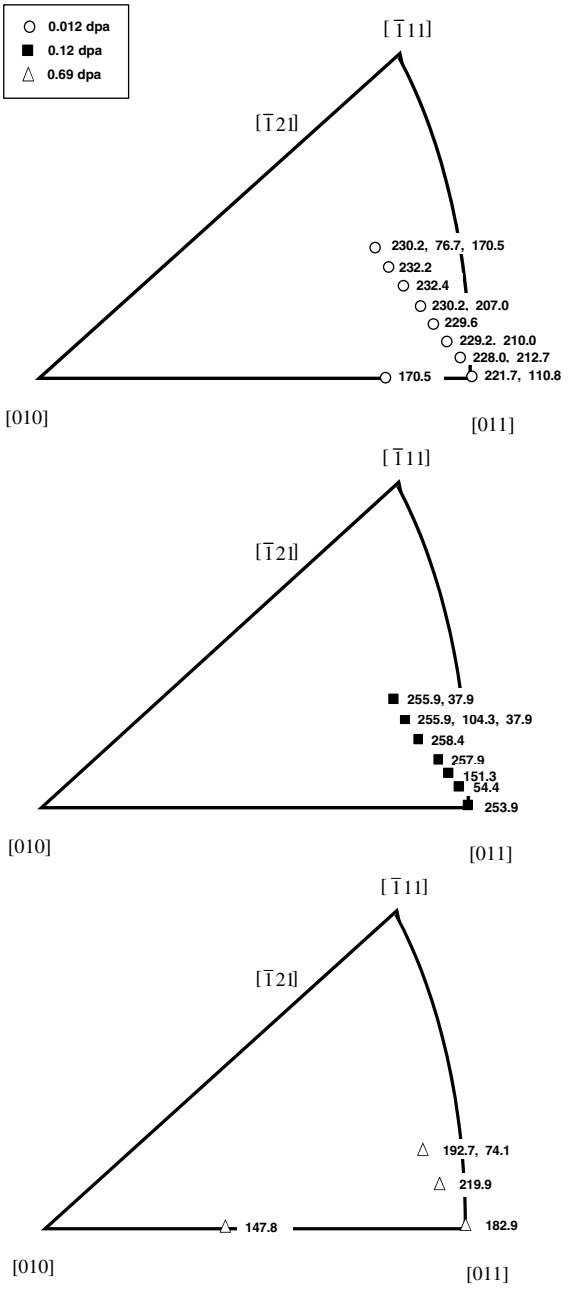

Fig. 5. Relationship between direction of the applied stress (tensile axis) in the channeling-occurred grain and the estimated resolved shear stress (MPa) for each channel.

The values of the resolved shear stress and channel width vary at each dose, so that no reasonable relationship can be found. Basically, channel width is not a measure of shear stress but shear strain, and also, channeling is plastic deformation, and highly heterogeneous deformation, therefore, there is not a simple relationship between stress and strain. However, relationship

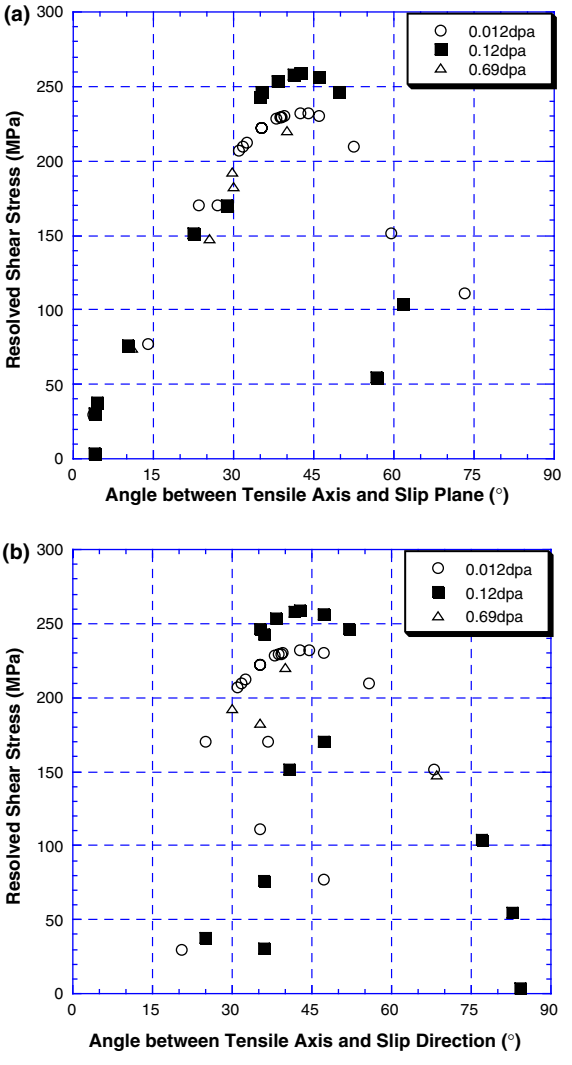

Fig. 6. Dependence of angle between tensile axis and slip plane normal (a) and slip direction (b) on resolved shear stress in each channeling-occurred grain.

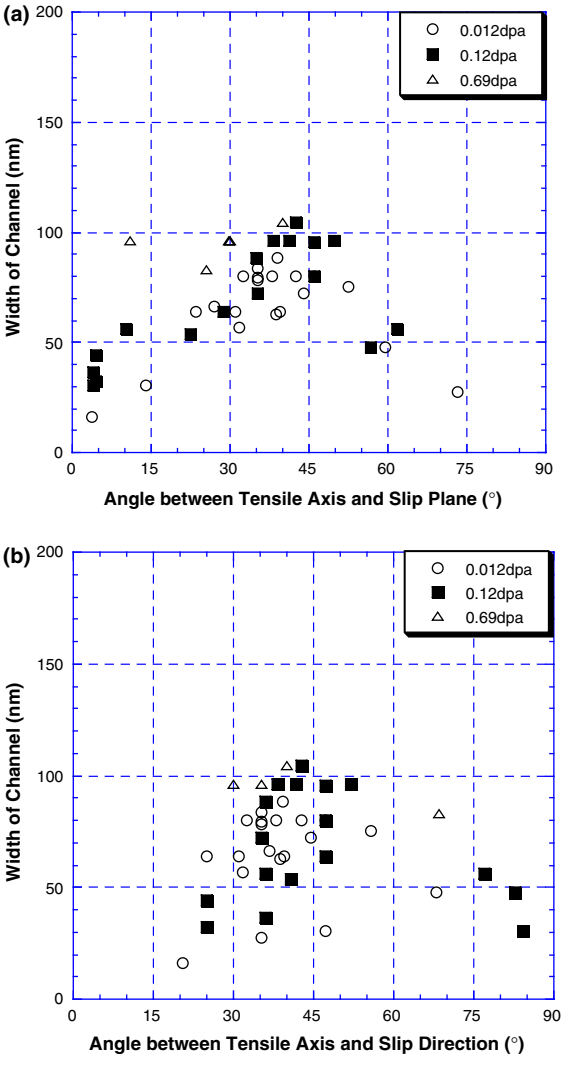

Fig. 7. Dependence of angle between tensile axis and slip plane normal (a) and slip direction (b) on channel width in each channeling-occurred grain.

between channel width and the resolved shear stress attracts an interest. As seen in Fig. 8, channel width increased with increasing the resolved shear stress at each dose, indicating the rapid deformation tends to occur at a high resolved shear stress level. In addition, it seemed that there is the dose dependence on the correlation between channel width and resolved shear stress, the slope of this correlation increased with increasing dose. This result suggests that at higher dose (higher density of irradiation-induced defect cluster) the rapid deformation could occur with locally forming wider dislocation channel due to high resolved shear stress.

A characteristic feature that accompanies the pronounced hardening in metals irradiated at ambient temperatures is the loss of work hardening capacity. Early studies of radiation hardening produced competing models for the hardening mechanism, based on the dislocation source locking and lattice friction. Several researchers have proposed that both mechanisms operate, with source hardening responsible for the upper yield point and lattice hardening responsible for the lower yield stress observed in metals irradiated at ambient temperatures [25–27]. The loss of work hardening capacity produces sharp decreases in uniform elongation. Both effects have been shown to be generally due to dislocation channeling [2,23,28–33]. Twinning has also been observed to cause a pronounced loss in strain hardening capacity in austenitic stainless steel irradiated at around 300 °C and tested near room temperature [34–37], however, no twinning was observed in the present

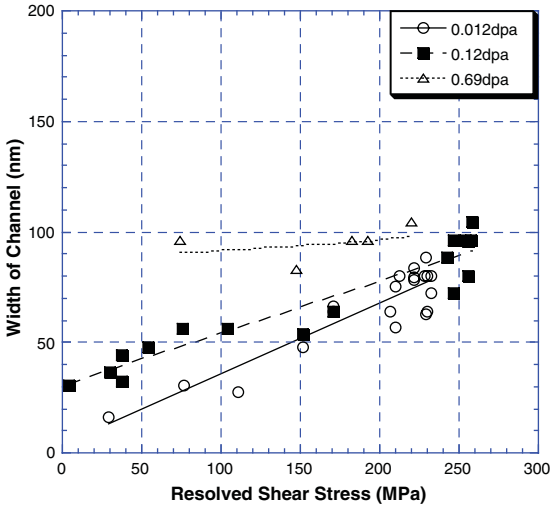

Fig. 8. Relationship between channel width and the resolved shear stress.

experiment. From these results, it is suggested that the loss of work hardening capacity in pure vanadium irradiated at low temperature could be mainly due to dislocation channeling locally formed with high resolved shear stress, leading to the rapid deformation.

4. Conclusions

The deformation microstructure of irradiated pure vanadium has been investigated by transmission electron microscopy in order to understand the deformation mechanisms of materials showing loss of strain hardening capacity. Dislocation pileup on grain boundary was observed in the deformed specimens irradiated to 0.012 dpa, indicating that the source of channeling could not be grain boundary only. TEM analysis suggested that there is a tendency that directions of the applied stress with greater resolved shear stress lie on the trace containing [0 1 1] and [1 1 2] directions. Channel width seems to be wider in case angle between tensile direction and dislocation slip direction is close to 45°. Furthermore, there is the dose dependence on the correlation between channel width and resolved shear stress, the slope of this correlation decreased with increasing dose. It is suggested that the loss of work hardening capacity in irradiated pure vanadium could be mainly due to dislocation channeling locally formed with high resolved shear stress.

Acknowledgment

This research was sponsored by the Division of Material Science and Engineering, the office of Basic Energy Sciences and by the office of Fusion Energy, US Department of Energy, under contract No DE-AC05-00OR22725 with UT-Battelle, LLC.

References

[1] T.J. Koppenaal, R.J. Arsenault, Metall. Rev. 16 (1971) 175.
[2] M.S. Wechsler, in: R.E. Reed-Hill (Ed.), In the Inhomogeneity of Plastic Deformation, American Society for Metals, Metals Park, OH, 1972, p. 19.
[3] M.J. Makin, in: Radiation Effects, in: W.F. Sheely (Ed.), Metallurgical Society Conference, Vol. 37, Gordon and Breach, New York, 1967, p. 627.
[4] J. Diehl, G.P. Seidel, in: Radiation Damage in Reactor Materials, Vol. I, IAEA, Vienna, 1969, p. 187.
[5] A.K. Seeger, in: 2nd UN Conference on Peaceful Uses of Atomic Energy, Vol. 6, United Nations, New York, 1958, p. 250.
[6] A.L. Bement Jr., in: W.C. Leslie (Ed.), 2nd International Conference on Strength of Metals and Alloys, Vol. II, American Society for Metals, Metals Park, OH, 1970, p. 693.
[7] J. Diehl, W. Schilling, in: 3rd International Conference on Peaceful Uses of Atomic Energy, Vol. 9, United Nations, New York, 1965, p. 72.
[8] J.C. Wilson, in: 2nd UN International Conference on Peaceful Uses of Atomic Energy, Properties of Reactor Materials, Vol. 5, United Nations, New York, 1958, p. 431.
[9] G.E. Lucas, J. Nucl. Mater. 206 (1993) 287.
[10] J.P. Robertson, R.L. Klueh, K. Shiba, A.F. Rowcliffe, Fusion Materials Semiannual Progress Report for period ending 31 December 1997, DOE/ER-0313/23, Oak Ridge National Lab, 1997, p. 179.
[11] S.J. Zinkle, L.L. Snead, A.F. Rowcliffe, D.J. Alexander, L.T. Gibson, Fusion Materials Semiannual Progress Report for period ending 30 June 1998, DOE/ER-0313/24, Oak Ridge National Lab, 1998, p. 33.
[12] K. Farrell, T.S. Byun, J.W. Jones, L.T. Gibson, R.G. Sitterson, N. Hashimoto, J.L. Bailey, M.J. Gardner, in: Gardner, Small Specimen Test Techniques: Fourth Volume, in: M.A. Sokolov, J.D. Landes, G.E. Lucas (Eds.), ASTM STP, Vol. 1418, ASTM International, West Conshohocken, PA, 2002.
[13] U.F. Kocks, Mater. Sci. Eng. 27 (1977) 291.
[14] S.J. Zinkle, Radiat. Eff. Def. Solids 148 (1999) 447.
[15] H. Matsui, O. Yoshinari, K. Abe, J. Nucl. Mater. 855 (1986) 114.
[16] R. Bajaj, M.S. Wechsler, in: M.T. Robinson, F.W. Young Jr. (Eds.), Fundamental Aspects of Radiation Damage in Metals, Vol. ll, CONF-751006-P2, National Tech. Inform. Service, Springfield, VA, 1975, p. 1010.
[17] K. Shiraishi, K. Fukaya, Y. Katano, in: S. Watson, F.W. Wiffen (Eds.), Radiation Effects and Tritium Technology for Fusion Reactors, Vol. ll, USERDA, Gatlinburg, TN, 1976, p. 122.
[18] E.R. Bradley, R.H. Jones, J. Nucl. Mater. 901 (1981) 103.
[19] S. Kojima, S.J. Zinkle, H.L. Heinisch, J. Nucl. Mater. 982 (1991) 179.

[20] Y. Dai, M. Victoria, in: Microstructure Evolution During Irradiation, in: I.M. Robertson et al. (Eds.), MRS Symposium Proceeding, Vol. 439, Materials Research Society, Pittsburgh, 1997, p. 319.
[21] S.J. Zinkle, R.L. Sindelar, J. Nucl. Mater. 1196 (1988) 155.
[22] N. Hashimoto, E. Wakai, J.P. Robertson, J. Nucl. Mater. 273 (1999) 95.
[23] P.M. Rice, S.J. Zinkle, J. Nucl. Mater. 1414 (1998) 258.
[24] N. Hashimoto, T.S. Byun, K. Farrell, S.J. Zinkle, J. Nucl. Mater. 329–333 (2004) 947.
[25] M.J. Makin, J.V. Sharp, Phys. Stat. Sol. 9 (1965) 109.
[26] B.N. Singh, A.J.E. Foreman, H. Trinkaus, J. Nucl. Mater. 249 (1997) 103.
[27] N. Baluc, C. Bailat, Y. Dai, M.I. Luppo, R. Schaublin, M. Victoria, in: Microstructural Processes During Irradiation, in: S.J. Zinkle et al. (Eds.), MRS Symposium Proceedings, Vol. 540, Materials Research Society, Warrendale, PA, 1999, p. 539.
[28] J.L. Brimhall, B. Mastel, Appl. Phys. Lett. 9 (1966) 127.
[29] J.V. Sharp, Philos. Mag. 16 (1967) 77.
[30] J.V. Sharp, Radiat. Eff. 14 (1972) 71.
[31] L.M. Howe, Radiat. Eff. 23 (1974) 181.
[32] A. Okada, K. Kanao, T. Yoshiie, S. Kojima, Mater. Trans. JIM 30 (1989) 265.
[33] A. Luft, Prog. Mater. Sci. 35 (1991) 97.
[34] N. hashimoto, S.J. Zinkle, A.F. Rowcliffe, J.P. Robertson, S. Jitsukawa, J. Nucl. Mater. 528 (2000) 283.
[35] S.M. Bruemmer, J.I. Cole, R.D. Carter, G.S. WasMRS Symposium Proceedings, Vol. 439, Materials Research Society, Warrendale, PA, 1997, p. 437.
[36] R.D. Carter, M. Atzmon, G.S. Was, S.M. BruemmerMRS Symposium Proceedings, Vol. 373, Materials Research Society, Warrendale, PA, 1995, p. 171.
[37] J.L. Brimhall, J.I. Cole, J.S. Vetrano, S.M. BruemmerMRS Symposium Proceedings, Vol. 373, Materials Research Society, Warrendale, PA, 1995, p. 177.